Open access • Journal Article • DOI:10.1049/IET-RPG.2009.0142

Coordinated output control of multiple distributed generation schemes

Samuel Jupe, Phil Taylor, Andrea Michiorri

Institutions: Durham University

Published on: 27 May 2010 - Iet Renewable Power Generation (Institution of Engineering and Technology (IET))

Topics: Distributed generation and Electric power system

Coordinated output control of multiple distributed generation schemes

S Jupe, P Taylor, Andrea Michiorri

Coordinated output control of multiple distributed generation schemes

S. C. E. Jupe, P. C. Taylor and A. Michiorri

School of Engineering
Durham University
South Road
Durham
DH1 3LE

s.c.e.jupe@durham.ac.uk
p.c.taylor@durham.ac.uk
andrea.michiorri@durham.ac.uk

Abstract: This paper presents candidate strategies for the coordinated output control of multiple distributed generation schemes. The proposed strategies are underpinned by power flow sensitivity factors and allow real-time knowledge of power system thermal ratings to be utilised. This could be of value in situations where distribution network power flows require management as a result of distributed generation proliferation. Through off-line open-loop simulations, using historical data from a section of the UK distribution network, the candidate strategies are evaluated against a benchmark control solution in terms of annual energy yields, component losses and voltages. Furthermore, the individual generator annual energy yields and generator-apportioned losses are used to assess the net present values of candidate control strategies to distributed generation developers.

Nomenclature

$C_{1,2,3}$	Variable costs (£M)
$C_{control}$	Cost of the distributed generator output control system (£M)

$C_{install}$	Total wind farm installation costs (£M/MW)
C_{inv}	Total investment cost for each distributed generation developer (£M)
C_{loss}	Cost of losses (£M)
C_{OM}	Cost of distributed generation annual operations and maintenance (£M)
$C_{real\text{-}time}$	Cost of real-time thermal rating system (£M)
C_{ROC}	Sale price of Renewables Obligation Certificates (£/MWh)
$C_{wholesale}$	Wholesale electricity price (£/MWh)
E_a	Metered annual energy yield of a distributed generator (MWh)
E_{loss}	Generator-apportioned annual energy loss (MWh)
G_i	Installed capacity of the wind farm (MW)
G_{id}	Unique identifier (*id*) of distributed generator, *G*
${}^{0,x,y}G_P$	Real power output of the generator at the initial (0), intermediate (*x*) and final (*y*) time-steps (MW)
$G_{P,m}$	Real power output of distributed generator, *G*, at node *m* (MW)
$'G_{P,m}$	Real power output of distributed generator, *G*, at node *m* before control actions have been implemented (MW)
$''G_{P,m}$	Real power output of distributed generator, *G*, at node *m* after control actions have been implemented (MW)
$\Sigma G_{P,m}$	Total real power injection at node *m* from multiple distributed generators (MW)
$\boldsymbol{J}$	Jacobian matrix of AC load flow
K	Proportionality factor
$\boldsymbol{M_{LIFO}}$	Matrix denoting the last-in first-off constraint order of distributed generation schemes
$\boldsymbol{M_{PFSF}}$	Matrix of power flow sensitivity factors

$\boldsymbol{M_{TMA}}$	Matrix denoting the technically most appropriate constraint order of distributed generation schemes
N	Number of stake-holder investors in control system
N-1	First circuit outage (electrical contingency)
NPV	Net present value (£M)
$\boldsymbol{P}$	Vector of real powers (MW)
${}^{0,x,y}P_{loss}$	Real power loss at the initial (0), intermediate (x) and final (y) time-steps (MW)
$P_{loss,i,k,m}$	Real power loss due to Joule effect heating (I^2R) in component between node i and node k and apportioned to a particular generator at node m (MW)
$P_{loss,i,k,total}$	Total real power loss due to Joule effect heating (I^2R) as heat in the component between node i and node k (MW)
PI	Profitability index
PV	Present value (£M)
$\boldsymbol{Q}$	Vector of reactive powers (MVAr)
$'Q_{i,k}$	Reactive power flowing from node i to node k before control actions have been implemented (MVAr)
$''Q_{i,k}$	Reactive power flowing from node i to node k after control actions have been implemented (MVAr)
R_a	Annual net revenue of each wind farm developer (£M)
R_{EY}	Annual revenue from metered active annual energy yield (£M)
$S_{i,k}^{lim}$	Thermal limit (static or real-time) of the component from node i to node k (MVA)

$'S_{i,k}$	Apparent power flowing from node i to node k before control actions are implemented (MVA)
$U_{i,k}$	Utilisation of component between node i and node k
U_{Tar}	Target utilisation of component after control actions have been implemented
$\boldsymbol{V}$	Vector of nodal voltages (kV)
$dP_{i,k} / dG_{P,m}$	Power flow sensitivity factor representing the change in real power flow from node i to node k due to change in real power output of generator connected to node m
i	Busbar node
k	Busbar node
m	Busbar node
n	Number of stakeholder investors in real-time thermal rating system
t	Integration time-step (h)
x	Ranked order of constraint for a distributed generator
$\Delta G_{P,m}$	Required change in real power output of the generator, G, at node m (MW)
$\Delta P_{i,k}$	Required change in real power flowing from node i to node k for network power flow management (MW)
Φ	Egalitarian broadcast reduction signal (%)
$\boldsymbol{\theta}$	Vector of nodal voltage angles (rad)
AuRA-NMS	Autonomous regional active network management system
AC	Alternating current
B	Busbar
C	Component

CAISO	Californian independent system operator
DG	Distributed generation
DNO	Distribution network operator
GSP	Grid supply point
LIFO	Last-in first-off
PFSF	Power flow sensitivity factor (defined as $dP_{i,k} / dG_{P,m}$)
ROC	Renewables Obligation Certificate
RTTR	Real-time thermal rating (defined as S^{lim})
SCADA	Supervisory, control and data acquisition
SPEN	ScottishPower EnergyNetworks
TMA	Technically most appropriate

1 Introduction

The impetus of governments, on an international scale, to move towards low-carbon economy targets has brought about the proliferation of distributed electricity generation [1]. However, as the capacity and number of distributed generation (DG) schemes grows, high levels of DG may lead to localised power flow issues within existing distribution networks. Therefore, a requirement is emerging for strategies to control DG power outputs to manage network power flows.

Last-in first-off (LIFO) control strategies for multiple DG schemes have been developed in the present regulatory framework of the UK. However, as the power transfer capacity of distribution networks becomes saturated, there is an economic disadvantage to ‘last-in’ generators. This is because they are the first generators to be disconnected or have their power output constrained at times of power flow management. The resulting annual energy yield of such generators may be significantly curtailed and, based on the anticipated net present value of the investment, the DG development may not be economically viable. This paper builds on previous work by the authors which described the underlying principles of DG output control for network power flow management [2] and candidate strategies for the output control of multiple generators [3] based on power flow sensitivity factors (PFSFs). PFSFs are derived from a full AC load flow solution and define the mathematical relationship between changes in network component power flows due to changes in DG power outputs. The candidate control strategies move away from piecemeal generator control systems to coordinate the power outputs of multiple generators in order to achieve aggregated benefits for power system stakeholders. Under certain conditions the strategies have the potential to facilitate improved individual and aggregated annual energy yields for separately owned DG schemes [3], when compared to a benchmark LIFO DG tripping strategy. In such circumstances the coordinated output control of distributed generators could enhance the revenue streams of ‘last-in’ generators to an extent that the investment in the installation is economically viable. Moreover, cross-payments could be set-up between generators to ensure that those generators that constrain their power output to manage network power flows, facilitating an aggregated annual energy yield gain, are remunerated.

In situations where a viable assessment is made, power flows may be managed through the deployment of a DG power output control system coupled with component real-time thermal ratings (RTTRs). The adoption of RTTR systems is particularly relevant in applications where strong correlations exist between the cooling effect of environmental conditions and electrical power flow transfers. For example where high power flows resulting from wind generation at high wind speeds can be accommodated since the same wind speed has a positive effect on overhead line or power transformer cooling [4]-[6].

The research described in this paper forms part of a UK government-funded project [7], in conjunction with AREVA T&D, Imass, PB Power and ScottishPower EnergyNetworks (SPEN), which aims to manage, actively, DG based on component thermal properties. The on-line control system compares component RTTRs with network power flows and produces set points that are fed back to the DG operator for implementation. A section of SPEN's distribution network has been selected for field trials where electrical and thermal monitoring equipment has been installed to allow open loop validation of the algorithms developed.

The paper is structured in the following way: Section 2 provides a survey of the current techniques adopted for the power output control of DG and outlines the background to control techniques based on PFSFs, informed by component thermal properties. Section 3 proposes three candidate strategies (LIFO, egalitarian and technically most appropriate) for the output control of DG based on PFSFs. Section 4 describes the generic forms of the techniques used to quantify the candidate control strategy evaluation parameters. Section 5 describes the off-line simulation of the candidate control strategies, implemented to manage power flows within a section of the UK power system. Simulation results are presented and discussed in Section 6 and the impact of the candidate control strategies on evaluation parameters is quantified.

Where appropriate, the results are expressed as marginal values based on a datum control strategy corresponding to a LIFO DG tripping approach deployed with component static ratings. In light of the findings, recommendations are made regarding the suitability of the control strategies for deployment with different component thermal rating systems. Section 7 discusses the use of PFSFs and the relative merits of the candidate strategies for DG output control.

2 Background

2.1 Current DG control approaches

In the UK, solutions for the power flow management of single distributed generators have been proposed by the Energy Networks Association [8] as a distillation of a report by the Distributed Generation Coordinating Group's Technical Steering Group [9]. DG power output control is achieved through network availability assessments by tripping (disconnection) or a demand-following strategy with auxiliary tripping. The latter strategy has the potential to utilise short-term component thermal ratings. Additionally, Roberts [10] considers the feasibility of incorporating the proposed solutions within a supervisory, control and data acquisition (SCADA) system for distribution network operators (DNOs).

Recent research investigates the constrained connection of multiple distributed generators on the island of Orkney [11]. A 'trim and trip' DG output control strategy is adopted and embedded in programmable logic control [12]. Reflecting present operational practices in the UK, a LIFO constraint priority defines the order in which generators are controlled.

As part of the AuRA-NMS project, Dolan *et al.* [13] present two techniques for the management of power flows within static thermal constraints. The techniques are illustrated through the control of DG within an 11kV distribution network and are assessed in terms of algorithm computational times and impact on DG curtailments. It is shown that the current-tracing technique marginally achieves the least DG real power curtailment but that the constraint satisfaction problem technique is more computationally efficient and allows contractual constraints to be considered.

Kabouris and Vournas [14] demonstrate the on-line development of interruptible wind farm contracts to manage the power flow through a congested corridor of the Hellenic Interconnected System in Greece. When security constraints are violated, the control of multiple DG schemes is achieved through the proportional reduction of generators' power output or by distributing generator curtailments according to a continuously updated priority list. Both proactive (pre-outage) and reactive (post-outage) control concepts are developed and illustrated based on a static security assessment of the available transfer capacity.

The concept of a delegated dispatch control centre has been developed in Spain to act as a mediator between the transmission system operator and a collection of wind farms connected to the same injection node [15]. Using a proactive control approach based on 15-minute operational forecasts, the delegated dispatch responds to system operator constraints imposed on the injection node. An optimisation problem is formulated considering power outputs of the generators, generator profit, busbar voltages and component thermal limits. In meeting the system operator constraints, the objective function aims to maximise generator aggregated profits.

Makarov *et al.* [16] investigate the operational impacts of increased wind generation within the Californian power system. Case study scenarios are modelled for the years 2006 (with 2.6GW installed capacity of wind generation) and 2010 (with anticipated 6.7 GW installed capacity of wind generation). The paper focuses on the forecasted difference between generation and load demand, and the required ramp rates of the generators to balance the power in real-time. Power flows are managed using a proactive control approach whereby hour-ahead and five-minute-ahead load and wind generation forecasts inform the California Independent System Operator (CAISO) Balancing Authority. This allows the CAISO to schedule and dispatch conventional generation to maximise the wind generation penetration.

The incorporation of overhead line RTTRs for the power output control of wind farm connections is presently being considered by Yip *et al.* [17]. In this distribution network application, the wind farm receives power output reduction signals if a power flow violation beyond the RTTR occurs. With auxiliary functionality, the wind farm is tripped to protect the overhead line if the power output is not reduced by the designated amount within the designated time-frame.

Supplementary relevant work regarding the methods of different generation types to achieve dispatched power set points is provided in [18]-[19] for wind turbines and [20] for hydro turbines. In addition, the strategic benefits of DG ownership for DNOs is discussed by Siano *et al.* in [21] and the authors conclude that incentives need to be put in place to encourage DG deployment for the benefit of the distribution network.

This paper adds to the work above by proposing candidate strategies for the coordinated output control of multiple DG schemes in order to manage power flows within multiple components of the distribution network. This is of relevance in situations where individual generators may cause power flow excursions in individual components but of particular relevance in situations where the aggregation of power flows from multiple generators may cause more widespread power flow management issues. Therefore, with the expected proliferation of DG the resulting power flows are likely to affect many components within the distribution network and it is important to take a holistic view of power flow management. Since this research project aims to develop and deploy an economically viable on-line control system, it is important that algorithms are developed with fast computational speeds and have the capability of utilising real-time information about the thermal status of the distribution network. Thus predetermined PFSFs are embedded within the control system for computational efficiency and a simulation tool is utilised to validate the control actions. Beyond the research described above, this paper also aims to quantify and compare the candidate strategies through a comprehensive set of evaluation parameters: DG individual and aggregated annual energy yields, generator-apportioned losses, DG development net present values and investment profitability indices, and busbar voltages. In addition, this paper also aims to quantify the impact of deploying the candidate strategies with different component rating systems, on the above mentioned evaluation parameters.

2.2 Power flow sensitivity factors

Underpinning this work is the theory of power flow sensitivity factors (PFSFs) that relate the changes in distribution network power flows to DG nodal power injections [2], [22]. The PFSFs are derived from the inverse Jacobian matrix, evaluated through a full AC load flow solution (1) [23].

$$\begin{bmatrix} \boldsymbol{\Delta\theta} \\ \boldsymbol{\Delta V} \end{bmatrix} = [\boldsymbol{J}]^{-1} \begin{bmatrix} \boldsymbol{\Delta P} \\ \boldsymbol{\Delta Q} \end{bmatrix} = \begin{bmatrix} \dfrac{\partial \boldsymbol{\theta}}{\partial \boldsymbol{P}} & \dfrac{\partial \boldsymbol{\theta}}{\partial \boldsymbol{Q}} \\ \dfrac{\partial \boldsymbol{V}}{\partial \boldsymbol{P}} & \dfrac{\partial \boldsymbol{V}}{\partial \boldsymbol{Q}} \end{bmatrix} \times \begin{bmatrix} \boldsymbol{\Delta P} \\ \boldsymbol{\Delta Q} \end{bmatrix} \tag{1}$$

Thus the PFSFs for a real power injection at node m are calculated from (2)-(3)

$$f(\theta): \frac{dP_{i,k}}{dG_{P,m}} = \left(\frac{\partial P}{\partial \theta}\right)_{i,k} \times \left(\frac{d\theta_k}{dG_{P,m}} - \frac{d\theta_i}{dG_{P,m}}\right) \tag{2}$$

$$f(V): \frac{dP_{i,k}}{dG_{P,m}} = \left(\frac{\partial P}{\partial V}\right)_{i,k} \times \left(\frac{dV_k}{dG_{P,m}} - \frac{dV_i}{dG_{P,m}}\right) \tag{3}$$

where $f(\theta)$ and $f(V)$ represent functions of nodal voltage angles and nodal voltage magnitudes respectively, $(dP/d\theta)_{i,k}$ and $(dP/dV)_{i,k}$ represent elements within the Jacobian matrix and $d\theta_i/dG_{P,m}$, $d\theta_k/dG_{P,m}$, $dV_i/dG_{P,m}$ and $dV_k/dG_{P,m}$ represent elements corresponding to the vector $\begin{bmatrix} \boldsymbol{\Delta\theta} \\ \boldsymbol{\Delta V} \end{bmatrix}$ evaluated in (1). For a given operating condition, the evaluated PFSFs may be stored efficiently in matrix form (4).

$$
\boldsymbol{M}_{\boldsymbol{PFSF}} = \begin{bmatrix} dP_{1,2}/dG_{P,1} & dP_{1,3}/dG_{P,1} & \cdots & dP_{i,k}/dG_{P,1} \\ dP_{1,2}/dG_{P,2} & dP_{1,3}/dG_{P,2} & \cdots & dP_{i,k}/dG_{P,2} \\ \vdots & \vdots & \ddots & \vdots \\ dP_{1,2}/dG_{P,m} & dP_{1,3}/dG_{P,m} & \cdots & dP_{i,k}/dG_{P,m} \end{bmatrix} \qquad (4)
$$

An assessment of the amount an individual generator is required to be constrained may be made using (5)-(6) and PFSF values from the matrix $\boldsymbol{M}_{\boldsymbol{PFSF}}$ (4).

$$
\Delta G_{P,m} = \frac{\Delta P_{i,k}}{\left(dP_{i,k}/dG_{P,m} \right)} \qquad (5)
$$

$$
\Delta P_{i,k} = \sqrt{\left(\left(U_{Tar} \times S_{i,k}^{lim} \right)^2 - \left({}^{\prime\prime}Q_{i,k} \right)^2 \right)} - \sqrt{\left(\left({}^{\prime}S_{i,k} \right)^2 - \left({}^{\prime}Q_{i,k} \right)^2 \right)} \qquad (6)
$$

Thus the updated generator output is evaluated using (7)

$$
{}^{\prime\prime}G_{P,m} = {}^{\prime}G_{P,m} + \Delta G_{P,m} \qquad (7)
$$

2.3 Component ratings

Due to the variability and unpredictability of meteorological conditions, fixed seasonal assumptions are used to determine component ratings, S^{lim}, which can be a conservative representation of actual operating conditions [6]. Difficulties associated with the maintenance of accurate seasonal rating databases often result in summer static rating utilisations throughout the year [10]. Moreover, the seasonal rating approach bears the latent risk of an anomalous ‘hot day’ where the prevailing meteorological conditions mean that components may be rated higher than they should be. For the purpose of this research, RTTRs are defined as a time-variant rating which can be practically exploited without damaging components or reducing their life expectancy. To calculate and exploit the RTTR, it is assumed that local environmental condition measurements are available as inputs to steady-state thermal models and that there are no outages (planned or unplanned) present within the electrical power system. Short-term transients, taking into account the thermal capacitance of power system components, are not included within the RTTR assessment. It is felt that this would not materially affect the GWh/annum throughput of energy within the electrical power system.

3 Proposed strategies for multiple DG control

This section presents the candidate strategies for power output control of multiple DG schemes.

3.1 LIFO PFSF-based

DG power outputs are curtailed in a LIFO contractual order, defined within the matrix $\boldsymbol{M_{LIFO}}$ (8)

$$\boldsymbol{M_{LIFO}} = \begin{bmatrix} x_1^{G_{id}} & x_2^{G_{id}} & \cdots & x_m^{G_{id}} \end{bmatrix} \quad (8)$$

where the integer x, represents the ranked order of DG curtailment for the generator, G, with a unique identifier (id), at nodes 1, 2, up to m respectively. The unique identifier aids clarity and is necessary for situations where multiple generators have the same connection point to the distribution network but separate operating contracts. The generic form of this strategy is given in (9)–(12). A set point change is dispatched to relevant DG operators that match DG power outputs to the capability of the network. If, by implementing the required reduction, as calculated in (9), the signal is driven negative (10) the DG is tripped (11) and the next generator, contractually, to be constrained is apportioned the required power output reduction (12). By adopting this approach, ‘last-in’ DG schemes are required to manage network power flows, when excursions occur, even though they may not technically be the most appropriate generators to do so.

$$ {}^{x}\Delta G_{P,m} = \frac{{}^{x}\Delta P_{i,k}}{{}^{x}\left(dP_{i,k} / dG_{P,m} \right)} \quad (9) $$

If:

$$ {}^{x}G_{P,m} + {}^{x}\Delta G_{P,m} < 0 \quad (10) $$

Then:

$$ {}^{x}G_{P,m} = 0 \quad (11) $$

and

$$ {}^{x+1}\Delta P_{i,k} = {}^{x}\Delta P_{i,k} - {}^{x}G_{P,m} \times {}^{x}\left(dP_{i,k} / dG_{P,m} \right) \quad (12) $$

3.2 Egalitarian broadcast

In this strategy a single percentage reduction signal, Φ, as calculated in (13)-(14), is broadcast to all the relevant generators. When calculating the reduction signal, the power outputs of each generator are weighted by the associated PFSFs. The constraints required to manage network power flows are shared by each generator and those generators making a significant power output contribution are constrained more, in terms of the absolute power output reduction (ΔG_P) than those generators making a small contribution.

$$\Delta G_{P,m} = G_{P,m} \times \Phi \quad (13)$$

$$\Phi = \frac{\Delta P_{ik}}{\sum_{m=0}^{m=\infty}\left(G_{P,m} \times \left(dP_{ik} / dG_{P,m}\right)\right)} \quad (14)$$

3.3 Technically most appropriate

The curtailment of the generators is ranked, in a technical priority order, by the relative magnitude of PFSFs given in matrix $\boldsymbol{M_{TMA}}$ (15)

$$\boldsymbol{M_{TMA}} = \begin{bmatrix} x_1^{G_{id}} & x_2^{G_{id}} & \cdots & x_m^{G_{id}} \end{bmatrix} \quad (15)$$

where the integer x, represents the ranked order of DG curtailment for the generator, G, with a unique identifier (id) at nodes 1, 2, up to m respectively, based on the relative magnitudes of PFSFs given in (4). The generic form of this strategy implementation is given in (9)–(12). In this case the DG with the best technical ability to manage network power flows is selected to be constrained first.

4 Quantification Techniques

In this section the techniques used to quantify the strategy evaluation parameters are given in generic forms. These include: numerical integration to calculate annual energy yields and annual energy losses, a loss apportioning technique to attribute energy losses to particular generators and the financial quantification of DG development net present values and profitability indices.

4.1 Numerical integration

The numerical technique used to integrate DG power outputs and hence quantify DG annual energy yields is given in (16)

$$E_a = t\left[\tfrac{1}{2}\left({}^{0}G_P + {}^{y}G_P \right) + \sum_{x=1}^{x=y-1} {}^{x}G_P \right] \qquad (16)$$

4.2 Loss apportioning

The technique used to apportion energy losses to individual generators in a proportional manner, through a component connecting multiple DG schemes to the distribution network, is given in (17)-(18)

$$P_{loss,i,k,m} = P_{loss,i,k,total} \times {G_{P,m}} \Big/ {\sum G_{P,m}} \qquad (17)$$

$$E_{loss} = t\left[\tfrac{1}{2}\left({}^{0}P_{loss} + {}^{y}P_{loss} \right) + \sum_{x=1}^{x=y-1} {}^{x}P_{loss} \right] \quad (18)$$

More complex loss apportioning techniques, looking deeper into the power system, are described by Bialek [24] for power flow tracing and by Kirschen and Strbac [25] for current tracing.

4.3 Financial assessment

Building on the work of Payyala and Green [26], the methodology used to evaluate the net present value of the wind farm investment to each DG developer, and therefore the profitability index, is presented.

The total investment cost for each developer, C_{inv}, is modelled as a sum of three variable costs (19)-(22)

$$C_{inv} = C_1(G_i) + C_2(N) + C_3(n) \quad (19)$$

where

$$C_1(G_i) = G_i \times C_{install} \quad (20)$$

and G_i represents the installed capacity of the wind farm and $C_{install}$ represents the total wind farm installation costs including wind turbine generators, foundations, electrical infrastructure, and planning and development costs;

$$C_2(N) = C_{control} / N \qquad (21)$$

where the cost of the control system, $C_{control}$, including development costs, installation costs, maintenance costs, necessary communication links and the auxiliary trip system is shared amongst the number of stakeholder investors (*N*) and

$$C_3(n) = C_{real-time} / n \qquad (22)$$

where the cost of the RTTR system, $C_{real\text{-}time}$, including development costs, thermal instrumentation costs, maintenance costs and the cost of necessary communication links is shared amongst the number of stakeholder investors, *n*.

The cost of the annual operations and maintenance, C_{OM}, is modelled as a proportion, *K*, of the wind farm installation cost (23)

$$C_{OM} = K \times G_i \times C_{install} \qquad (23)$$

The annual net revenue, R_a, of each wind farm developer is modelled (24)-(26) by subtracting the cost of losses, C_{loss}, from the metered active annual energy yield revenue, R_{EY}

$$R_a = R_{EY} - C_{loss} \quad (24)$$

$$R_{EY} = E_a \times \left(C_{wholesale} + C_{ROC}\right) \qquad (25)$$

$$C_{loss} = E_{loss} \times C_{wholesale} \quad (26)$$

Therefore the net present value (*NPV*) of each wind farm investment is quantified (27) by assessing the present value (*PV*) of the annuity ($R_a - C_{OM}$), discounted over the project lifetime, and subtracting the cost of the original investment.

$$NPV = PV(R_a - C_{OM}) - C_{inv} \quad (27)$$

The profitability index (*PI*) for each DG developer is defined as the ratio of the *NPV* to the initial investment (28) [26]

$$PI = {}^{NPV}\!/_{C_{inv}} \quad (28)$$

Clearly the results of financial evaluations are sensitive to wind farm installation costs, discount rates, project lifetimes, wholesale electricity prices and the sale price of ROCs. In quantifying the *NPV*s and *PI*s a discount factor of 10% was assumed for a 20-year operational lifetime of the wind farm [27], the wholesale electricity price was assumed to be £52.15/MWh [28] and the trading price of ROCs was assumed to be £49.28/MWh [29]. The cost of the offshore wind farm installation was assumed to be £1000/kW and the costs of the onshore wind farm installations were assumed to be £800/kW [30]. Wind farm annual operations and maintenance costs were assumed to be 5% of the wind farm installation cost [31]. The cost of the power output control system (including project management and engineering design, hardware, software, installation, testing, commissioning and maintenance) was estimated to be £200k with the incorporation of component thermal monitoring equipment and £100k without.

5 Case Study

5.1 Network description

A section of ScottishPower EnergyNetworks' distribution network, selected for RTTR field trials, is given in Figure 1 [32]. Additional generation was introduced at nodes B4 and B9 representing planned future connections of DG. Each DG scheme is separately owned and it was assumed that the generators' connection agreements contain the necessary clauses to allow operation outside of a LIFO constraint priority. A summary of DG types and installed capacities is given in Table 1. An underlying meshed 33kV network was included in the network model for simulations but for simplicity is not presented. Through an off-line analysis of the network (which entailed the simulation of the generators with unconstrained outputs throughout the year), power flow excursions, with static thermal ratings, were found to occur in overhead line components C3, C5, C6, C7, C8 and C9. These components have been highlighted in Figure 1. The majority of overloads are caused by high wind generation, which can occur at high and low loads. Current levels of DG, operated with static thermal ratings, at present have a very small probability of causing overloads unless N-1 conditions are encountered. However, this work assesses overloads when considering planned future DG connections where the anticipated growth of DG increases, significantly, the probability of overloads occurring for system-intact operation with static thermal ratings.

5.2 Control approach

Rule-based decision making (inference) is an artificial intelligence technique [33] which has the potential to facilitate the automated control of systems. In this case the rule-based inference engine is designed to support the control decisions of DNOs. For the field trial network operating in normal conditions, the PFSF matrix ($\boldsymbol{M_{PFSF}}$) was found to be of the form (29), based on the generalised matrix in (4). From left to right across each row, the terms relate to components C3, C5, C6, C7, C8 and C9. From top to bottom in each column the terms relate to DG7, DG8, DG1, DG2, DG3, DG4, DG5 and DG6.

$$\boldsymbol{M_{PFSF}} = \begin{bmatrix} dP^{C3}_{B3,B4}/dG_{P,B4} & 0 & dP^{C6}_{B5,B7}/dG_{P,B4} & dP^{C7}_{B7,B8}/dG_{P,B4} & dP^{C8}_{B5,B8}/dG_{P,B4} & 0 \\ 0 & dP^{C5}_{B5,B6}/dG_{P,B6} & dP^{C6}_{B5,B7}/dG_{P,B6} & dP^{C7}_{B7,B8}/dG_{P,B6} & dP^{C8}_{B5,B8}/dG_{P,B6} & 0 \\ 0 & 0 & dP^{C6}_{B5,B7}/dG^{1}_{P,B9} & dP^{C7}_{B7,B8}/dG^{1}_{P,B9} & dP^{C8}_{B5,B8}/dG^{1}_{P,B9} & dP^{C9}_{B5,B9}/dG^{1}_{P,B9} \\ 0 & 0 & dP^{C6}_{B5,B7}/dG^{2}_{P,B9} & dP^{C7}_{B7,B8}/dG^{2}_{P,B9} & dP^{C8}_{B5,B8}/dG^{2}_{P,B9} & dP^{C9}_{B5,B9}/dG^{2}_{P,B9} \\ 0 & 0 & dP^{C6}_{B5,B7}/dG^{3}_{P,B9} & dP^{C7}_{B7,B8}/dG^{3}_{P,B9} & dP^{C8}_{B5,B8}/dG^{3}_{P,B9} & dP^{C9}_{B5,B9}/dG^{3}_{P,B9} \\ 0 & 0 & dP^{C6}_{B5,B7}/dG^{4}_{P,B9} & dP^{C7}_{B7,B8}/dG^{4}_{P,B9} & dP^{C8}_{B5,B8}/dG^{4}_{P,B9} & dP^{C9}_{B5,B9}/dG^{4}_{P,B9} \\ 0 & 0 & dP^{C6}_{B5,B7}/dG^{5}_{P,B9} & dP^{C7}_{B7,B8}/dG^{5}_{P,B9} & dP^{C8}_{B5,B8}/dG^{5}_{P,B9} & dP^{C9}_{B5,B9}/dG^{5}_{P,B9} \\ 0 & 0 & dP^{C6}_{B5,B7}/dG^{6}_{P,B9} & dP^{C7}_{B7,B8}/dG^{6}_{P,B9} & dP^{C8}_{B5,B8}/dG^{6}_{P,B9} & dP^{C9}_{B5,B9}/dG^{6}_{P,B9} \end{bmatrix} \quad (29)$$

Furthermore, the LIFO DG constraint matrix ($\boldsymbol{M_{LIFO}}$) and the technically most appropriate DG constraint matrix ($\boldsymbol{M_{TMA}}$) were found to be of the form (30).

$$
M_{LIFO,TMA} = \begin{bmatrix} x_{B4}^{DG7} & 0 & x_{B4}^{DG7} & x_{B4}^{DG7} & x_{B4}^{DG7} & 0 \\ 0 & x_{B6}^{DG8} & x_{B6}^{DG8} & x_{B6}^{DG8} & x_{B6}^{DG8} & 0 \\ 0 & 0 & x_{B9}^{DG1} & x_{B9}^{DG1} & x_{B9}^{DG1} & x_{B9}^{DG1} \\ 0 & 0 & x_{B9}^{DG2} & x_{B9}^{DG2} & x_{B9}^{DG2} & x_{B9}^{DG2} \\ 0 & 0 & x_{B9}^{DG3} & x_{B9}^{DG3} & x_{B9}^{DG3} & x_{B9}^{DG3} \\ 0 & 0 & x_{B9}^{DG4} & x_{B9}^{DG4} & x_{B9}^{DG4} & x_{B9}^{DG4} \\ 0 & 0 & x_{B9}^{DG5} & x_{B9}^{DG5} & x_{B9}^{DG5} & x_{B9}^{DG5} \\ 0 & 0 & x_{B9}^{DG6} & x_{B9}^{DG6} & x_{B9}^{DG6} & x_{B9}^{DG6} \end{bmatrix} \quad (30)
$$

$\boldsymbol{M_{PFSF}}$ was populated as given in (31) [2].

$$
M_{PFSF} = \begin{bmatrix} -0.99 & 0 & 0.46 & 0.46 & 0.47 & 0 \\ 0 & -0.95 & 0.46 & 0.47 & 0.47 & 0 \\ 0 & 0 & 0.41 & 0.41 & 0.42 & -0.91 \\ 0 & 0 & 0.42 & 0.43 & 0.43 & -0.92 \\ 0 & 0 & 0.42 & 0.42 & 0.43 & -0.92 \\ 0 & 0 & 0.43 & 0.43 & 0.44 & -0.94 \\ 0 & 0 & 0.43 & 0.43 & 0.44 & -0.94 \\ 0 & 0 & 0.45 & 0.45 & 0.46 & -0.98 \end{bmatrix} \quad (31)
$$

$\boldsymbol{M_{LIFO}}$ is given in (32), based on (8) and DG contractual mechanisms. In addition, $\boldsymbol{M_{TMA}}$ is given in (33), based on (15) and (31).

$$
M_{LIFO} = \begin{bmatrix} 1 & 0 & 7 & 7 & 7 & 0 \\ 0 & 1 & 8 & 8 & 8 & 0 \\ 0 & 0 & 1 & 1 & 1 & 1 \\ 0 & 0 & 2 & 2 & 2 & 2 \\ 0 & 0 & 3 & 3 & 3 & 3 \\ 0 & 0 & 4 & 4 & 4 & 4 \\ 0 & 0 & 5 & 5 & 5 & 5 \\ 0 & 0 & 6 & 6 & 6 & 6 \end{bmatrix} \quad (32)
$$

$$M_{TMA} = \begin{bmatrix} 1 & 0 & 2 & 2 & 2 & 0 \\ 0 & 1 & 1 & 1 & 1 & 0 \\ 0 & 0 & 8 & 8 & 8 & 6 \\ 0 & 0 & 7 & 7 & 7 & 5 \\ 0 & 0 & 6 & 6 & 6 & 4 \\ 0 & 0 & 5 & 5 & 5 & 3 \\ 0 & 0 & 4 & 4 & 4 & 2 \\ 0 & 0 & 3 & 3 & 3 & 1 \end{bmatrix} \qquad (33)$$

Therefore a series of 'If-Then' rules were created to establish the relationship between the power system components and the generators that it would be necessary to constrain to manage network power flows.

Considering (31), the zero terms in the matrix represent a negligible PFSF and indicate that the power output of a generator has negligible impact on the power flows in that particular component. By inspection of this matrix it is possible to see that the power flows in components C3 and C5 are affected only by generation at nodes B4 and B6 respectively. This is a fairly intuitive finding as these components are the feeder connections for the relevant distributed generators. Moreover, the power flow in component C9 is sensitive only to the outputs of generators connected at node B9. Considering components C6, C7 and C8 it can be seen from Figure 1 that this is where power flows from all the distributed generators accumulate. Therefore the power flows in these components are sensitive to outputs from each distributed generator connected. Having identified these relationships the necessary rule-bases were created for the candidate control strategies. Considering Figure 1, an example rule-base is given in (34)-(37) for the necessary multiple DG constraints when implementing the egalitarian control strategy.

$$\begin{aligned}&\text{If}: U^{C6}_{B5,B7} > 1\\&\text{Then}: \text{Constrain DG1} - \text{DG8}\end{aligned} \qquad (34)$$

$$\begin{aligned}&\text{If}: U^{C7}_{B7,B8} > 1\\&\text{Then}: \text{Constrain DG1} - \text{DG8}\end{aligned} \qquad (35)$$

$$\begin{aligned}&\text{If}: U^{C8}_{B5,B8} > 1\\&\text{Then}: \text{Constrain DG1} - \text{DG8}\end{aligned} \qquad (36)$$

$$\begin{aligned}&\text{If}: U^{C9}_{B9,B5} > 1\\&\text{Then}: \text{Constrain DG1} - \text{DG6}\end{aligned} \qquad (37)$$

where U represents the utilisation of a particular component and is defined as the ratio of apparent power flow to the thermal limit ('$S_{i,k}$ / S^{lim}) and S^{lim} could be a static or real-time thermal rating.

5.3 Simulation approach

As a step towards the on-line control of multiple DG schemes, an off-line analysis was conducted to quantify the impact of the candidate control strategies on the evaluation parameters. Simulations used electrical data for the complete calendar year 2006, with a half-hourly data resolution. In order to reflect an element of diversity in the power injections, three different wind farm output profiles (two onshore and one offshore) were used for the analysis, each supplied by SPEN and based on historical data from the region being considered. DG1, DG2, DG3 and DG6 were modelled with one onshore profile, DG4 and DG5 were modelled with the other onshore profile and

DG7 and DG8 were modelled with the offshore profile. These profiles were scaled by the relevant installed capacities to represent the future DG power outputs. The control system simulation, as shown in Figure 2, functions in the following manner:

1. Grid supply point (GSP) reference voltages and power flows are input to the 'distribution network simulator' and 'offline simulation tool' both of which are load flow algorithms (a);
2. Normalised historical load demand and generation power output profiles are scaled through multiplication by peak values (b)-(c) respectively, which are also input to the 'distribution network simulator' and 'offline simulation tool' (d)-(e);
3. Component static and real-time thermal ratings are fed into the 'rule-based inference engine' (f) together with a full set of component power flows which have been computed by the 'distribution network simulator' (g). Based on the ranked magnitude of component utilisations together with embedded knowledge of the ability of DG to control component power flows (signified by non-zero values within $\boldsymbol{M_{PFSF}}$), the 'rule-based inference engine' decides if a control action is necessary and which DG scheme(s) should be constrained. If a control action is required then the $\Delta P_{i,k}$ value is passed to the 'DG set point calculator' (h). If no action is required then the 'offline analysis tool' records the present DG power outputs, component losses, component utilisations and busbar voltages (k) and the control system reads in data for the next ½ hour interval;
4. The 'DG set point calculator' receives information from the 'rule-based inference engine' regarding the necessary real power flow reduction as well as

an indication of which DG schemes have the ability to manage the network power flows. Using a look-up table of predetermined PFSFs ($\boldsymbol{M_{PFSF}}$), updated DG set points are calculated depending on the candidate control strategy selected;

5. New DG set point values are passed to the ‘offline simulation tool’ (i) and together with GSP reference voltages, reference power flows and load demands, an updated load flow is computed; and
6. The updated sets of complete power flows and busbar voltages are passed back to the inference engine (j). This validates that all power flows and voltages are within designated limits. Steps 3 – 6 are repeated with the updated DG set point values until all the power flows within the network are brought back within thermal limits.

In the simulated deployment of the candidate control strategies within the field trial network, the topology and generator installed capacities were assumed to be constants of the system. Component ratings, types, cross-sectional areas and maximum operating temperatures are summarised in Table 2. Component RTTRs were computed with a half-hourly data resolution for the calendar year 2006 using the thermal models described in [6] and historical meteorological data for the ‘Valley’ area of Wales, UK [34]. Simulations were conducted with a target utilisation, U_{Tar} = 0.95 and, rather than neglecting MVAr flow, it was assumed constant for a particular operating condition. Thus $dP/dG_P >> dQ/dG_P$ and a simplification was made to (6) that *“Q* ≈ *‘Q* [2].

6 Discussion of results

Based on the datum annual energy yield values in Table 1 together with Figures 3a-3b, the adoption of egalitarian and TMA control strategies is particularly favourable for 'last-in' generators DG1-4 in terms of increased annual energy yields and hence revenue stream enhancement. Considering Figure 3a, the egalitarian control strategy deployed with component static ratings facilitates increased annual energy yields of 83.6% (25.8GWh), 45.7% (21.3GWh), 23.6% (16.9GWh) and 13.7% (12.0GWh) for DG1-4 respectively, through the reduction in annual energy yields of DG5 and DG6 by 7.4% (8.4GWh) and 10.5% (11.9GWh) respectively. The TMA control strategy facilitates increased annual energy yields of 116.6% (36.0GWh), 71.9% (33.6GWh), 45.9% (32.8GWh) and 31.3% (27.5GWh) for DG1-4 respectively, through the reduction in annual energy yields of DG5 and DG6 by 18.0% (20.6GWh) and 29.5% (33.6GWh) respectively. Considering Figure 3b, for each control strategy deployment with RTTRs, every generator sees an energy yield gain, and hence revenue stream enhancement. The only exception to this is DG6, if the TMA strategy is adopted. In this case there is a marginal 3.2% reduction in the annual energy yield of the DG scheme, when compared to the datum value of 113.9GWh in Table 1. As seen in (31), DG5 and DG6 have higher PFSFs, relative to DG1-DG4, therefore they are, technically, the most appropriate generators to constrain in order to manage power flows within C9.

Considering Table 3, based on the datum value of 943.8GWh/annum, by inspection of the data in each column it is possible to observe the aggregated annual energy yield gains that may be achieved by the adoption of more sophisticated candidate PFSF-based control strategies, deployed with the specified component thermal rating system. Similarly, by inspection of each row it is possible to observe the aggregated annual energy yield gains that may be achieved by adopting a more sophisticated component thermal rating system, deployed with the specified control strategy. Respective aggregated annual energy yield gains of 6.5%, 7.1% and 11.0% may be achieved by the adoption of LIFO PFSF-based, egalitarian and TMA control strategies deployed with component static ratings. Therefore, the impact that coordinated power output control approaches have on individual generator revenue streams could mean that, even if the 'first-in' generators are remunerated for curtailing their power output at certain times of the year, there is an overall revenue gain for all the generators. Aggregated annual energy yield gains of 20.1% and 21.0% may be achieved by the respective adoption of basic DG tripping and the TMA control strategies deployed with component RTTRs. This represents increased aggregated energy yield of 190.1GWh/annum and 198GWh/annum beyond the datum value. As the component thermal rating system becomes more sophisticated the distinction between aggregated energy yields for the different candidate control strategies becomes less pronounced. However, the increased power transfer capacity that may be unlocked through component RTTR systems could lead to the accommodation of a larger installed capacity of distributed generation [6]. Therefore the adoption of coordinated DG power output control strategies could allow a greater percentage of the additional power transfer headroom to be realised.

The energy losses in C3 were apportioned directly to DG7, the losses in C5 were apportioned directly to DG8 and the losses in C9 were apportioned directly to DG1-6, based on (17)-(18) in Section 4.2. As seen in Figure 4a, DG1-4 are apportioned additional annual energy losses (291MWh, 252MWh, 219MWh and 177MWh respectively) when the egalitarian control strategy is adopted. Additional annual energy losses of 421MWh, 409MWh, 423MWh and 380MWh are attributed to DG1-4 respectively in deploying the TMA control strategy. Inspection of Figure 4b shows that further additional annual energy losses are apportioned to all the generators in deploying the candidate control strategies with component RTTRs. The increase in losses resulting from coordinated control strategies are a direct result of increased power transfers and hence increased energy yields of the generators.

Tables 4 and 5 summarise DG investment *NPV*s and *PI*s for the candidate control strategies deployed with component static and real-time thermal ratings respectively. An *NPV* < 0 indicates an investment is not financially viable. Moreover, in evaluating the impact of candidate control strategies on the financial performance of the DG developments, a *PI* > 1 could be specified as the investment criterion. This indicates that the investor will recover at least double the cost of the initial investment over the project lifetime.

Considering the results presented in Table 4 for the LIFO DG trip control approach, it can be seen that if this approach is adopted then the investment would not be viable for DG1 since the *NPV* of the development is £-0.9M. This is because DG1 represents the last generator to connect to the network and therefore the first generator to be disconnected at times of network power flow management. The resulting impact on the annual energy yield of the generator means that insufficient revenue is earned over the project lifetime to justify the initial investment cost. The LIFO PFSF-based approach is most preferable for DG5-8, in terms of revenue stream enhancement (with respective *NPV* gains of £34.4M, £33.8M, £105.8M and £151.6M.), since they are the 'first-in' generators. The egalitarian strategy enhances the revenue streams and hence increases the profitability indices of DG1-4 and DG7. The respective *NPV* gains for these generators were £41.4M, £42.3M, £45.7M, £42.3M and £112.2M. The technically most appropriate control strategy resulted in the greatest enhancement to the revenue streams of DG1-4 (with respective *NPVs* of £49.2M, £58.6M, £76.2M and £85.5M), due to the coordinated power output control of DG5-8 at times of power flow management. Considering Table 5, it can be observed that the candidate control strategies deployed with component RTTRs all display a similar financial performance (the largest *NPV* difference being £8.6M for DG6 without remuneration). The LIFO PFSF-based strategy is marginally favourable for DG5–8 (with respective profitability indices of 1.9, 2.4, 1.8 and 1.8) and the technically most appropriate strategy is marginally favourable for DG1–4 (with respective *PI*s of 2.4, 2.3, 2.4 and 2.6).

In all cases the busbar voltages conformed to the statutory UK requirements specified in [35]. Furthermore, for the simulated year, the voltage profiles of the busbars at the GSPs represented the extremities of voltage excursions away from nominal and all other busbar voltages remained within these bounds. The maximum per unit voltage difference between the LIFO DG tripping approach and the TMA strategy, deployed with component static thermal ratings, occurred at node B9 and was found to be 0.4%. This was attributed to a voltage rise effect [36] along the feeder. The maximum per unit voltage difference between TMA strategy deployments with component static and RTTRs also occurred at node B9 and was found to be 0.9%.

7 Discussion of control parameters and approaches

The proposed control techniques make use of predetermined PFSFs which have been shown to be a valid linear approximation of the network power flow management problem [2]. As seen in (5) there is an inverse relationship between the magnitude of PFSFs and the extent to which generators are constrained in order to manage network power flows. PFSFs are a function of the complex impedances of components within the electrical network as embodied in the Jacobian matrix. The connection of DG to electrically strong distribution networks with low impedance paths lead to high PFSFs. In weaker electrical networks, such as those found in rural parts of the UK, the long electrical feeders result in high electrical impedances. As a result there are greater electrical losses and lower PFSFs.

Distribution network topology changes have the potential to impact on the continued operation of the DG output control system particularly if the magnitude of PFSFs is affected. The derived PFSFs are network topology and network configuration specific and, in simulating the proposed control strategies it was assumed that the network topology was constant. It is feasible, however, to develop PFSF-based control strategies that make use of alternative sets of the above-mentioned predetermined PFSFs, based on network switch information. For each configuration a new off-line analysis would be required to determine the PFSFs. Alternatively, PFSFs could be calculated in real-time and used to update values within the control matrix $\boldsymbol{M_{PFSF}}$.

Network extensions and new DG connections are planned by the DNO many months in advance. The off-line methodology required to adapt the DG output control system to deal with these network topology changes is provided in [2]. An overview of the required control system modification is outlined below:

1. Modify the topology of the network, as appropriate, in the off-line analysis software and on-line simulation tool;
2. Conduct an new off-line study to identify any new thermally vulnerable components within the distribution network;
3. Develop, as appropriate, a new real-time thermal rating system to incorporate new thermally vulnerable components; and
4. Specifically related to the control algorithm, each control strategy would require updating in the following manner:
    a. Determine updated PFSFs;
    b. Modify the rule-base in the inference engine to achieve desired control functions;
    c. Incorporate additional terms in the DG set point calculator equations; and
    d. Update the on-line simulation tool to maintain the integrity of the power flow and voltage validation tasks.

It should be noted that some network topology changes may have a negligible impact on the magnitude of PFSFs and therefore control system modifications may not be necessary.

It is anticipated that the utilisation target, U_{Tar}, would be defined by the DG developer or DNO to represent the factor of safety, or risk, that the DNO is prepared to accommodate in terms of operating the relevant power system component. To minimise the risk of power flow excursions beyond the transfer capacity of components, and thus to ensure the safe and secure operation of the distribution network, it is expected that the candidate control strategies would be deployed with an auxiliary trip system [17]. With the functionality to incorporate the same component rating systems as the primary control system, the auxiliary system acts as a backup in the case of control system operation failure, communications failures or the failure of DG schemes to match the updated set points within the required time frame.

The DG output control system makes use of an on-line simulation tool that has the capability of validating operational voltages against operational limits. If voltage limits were to become a constraining factor, this would currently need to be dealt with outside of the jurisdiction of the DG output control system using active voltage techniques as demonstrated in [37]. Alternatively, the functionality of the control system could be extended to make use of voltage sensitivity factors, as discussed in [23, 38]. The work in [38] is of particular relevance as it considers the coordinated output control of multiple DG schemes by use of voltage sensitivity factors.

LIFO strategies represent the present UK practice whereby 'last-in' generators are constrained for network power flow management. If management issues become more widespread 'last-in' generators may not be, technically, the most appropriate to constrain. Moreover, there is an increased complexity for DNOs in terms of dispatching constraint signals. The egalitarian broadcast strategy overcomes signal dispatching complexities. All technically relevant generators are controlled to manage network power flows and this has the potential to facilitate aggregated annual energy gains. The TMA strategy utilises generators with the best technical ability to manage network power flows. This has the potential to lead to the greatest aggregated annual energy yield gains of the proposed PFSF-based strategies. However, there is an associated signal dispatching complexity as DG proliferates and network management issues become more widespread. In situations where the PFSFs are of similar magnitude there is little merit in applying the technically most appropriate control strategy. However, the egalitarian strategy would still have the potential to allow increased installed capacities of intermittent generation thereby impacting on both individual and aggregated annual energy yields.

The control system uses the DNO's SCADA signals for electrical monitoring and DG output control. Therefore, moving from LIFO-based to non-LIFO-based control strategies has no added communication requirements when deployed with static thermal ratings. The step which would entail extra communication links is the implementation of RTTR systems. In research, also carried out Durham University as part of this project, thermal state estimation techniques have been developed and validated to estimate RTTRs in wide areas of the distribution network based on limited monitoring equipment and communication link installations [39].

8 Conclusions

This paper attempts to quantify the benefits in adopting candidate PFSF-based strategies for the future coordinated output control of multiple distributed generators. It is shown that, in certain circumstances, there are significant benefits to individual generators in terms of energy yields and hence revenue streams by moving away from LIFO control strategies. As a result the aggregated annual energy yield of separately owned generators is considerably improved. The impact that coordinated power output control approaches have on individual generator revenue streams could mean that, even if the ‘first-in’ generators are remunerated for curtailing their power output at certain times of the year, there is an overall revenue gain for all the generators.

Although the case study presented in this paper is UK-based, the strategies, simulation approach and research outcomes are transferable to networks internationally. Whilst, in the UK there are no mechanisms in place at present to encourage and reward an increase in aggregated energy yield contributions from separately owned distributed generations, there are examples in Europe where this concept is recognised and is beginning to be adopted [14]-[15].

Clearly, the illustrative figures, relating to financial assessments, vary with time and location. Variations in wind farm installation and operating costs would impact on the *NPV*s and *PI*s of the DG scheme developments, and hence the investment decision. If these values were to differ from the illustrative costs used in this paper, the principle of the analysis would still remain valid. The proposed methodology may be used with figures that are most appropriate to the particular situation being considered.

In light of the results and discussions presented in this paper, it is recommended that any DNO or DG developer looking to adopt the proposed PFSF-based strategies should conduct an off-line analysis to assess the value of output control of multiple DG schemes. This is because the control strategy implementations are a function of a number of site-specific control variables and therefore the economic value in each case is different. Work is continuing in this area to realise the potential of coordinated output control strategies for multiple DG schemes.

9 Acknowledgements

This work was supported by AREVA T&D, Imass, PB Power and ScottishPower EnergyNetworks with funding from the Department for Innovation, Universities and Skills, the UK Engineering and Physical Sciences Research Council and Durham University.

10 References

1 Strbac, G.: 'Electric power systems research on dispersed generation', *Electr. Power Syst. Res.*, 2007, **77**, (9), pp. 1143-1147

2 Jupe, S. C. E., Taylor, P. C.: 'Distributed generation output control for network power flow management', *IET Proc. RPG.*, 2009, **3**, (4), pp. 371-386

3 Jupe, S. C. E., Taylor, P. C.: 'Strategies for the control of multiple distributed generation schemes', Proc. 20th Int. Conf. Electricity Distribution, Prague, CZ, 8–11 June 2009

4 Belben, P. B., Ziesler, C. D.: 'Aeolian uprating: how wind farms can solve their own transmission problems', Proc. World Wind Energy Conference, Berlin, Germany, July 2002

5 Helmer, M.: 'Optimized size of wind power plant transformer and parallel operation', Proc. Wind Power for the 21st century, Kassel, Germany, 2000

6 Michiorri, A., Taylor, P. C., Jupe, S. C. E., Berry, C. J.: 'An investigation into the influence of environmental conditions on power system ratings', *Proc. IMechE - Part A: J. Power and energy*, 2009, **227**, (A7), pp. 743-757

7 Neumann, A., Taylor, P. C., Jupe, S. C. E., *et al.*: ‘Dynamic thermal rating and active control for improved distribution network utilization’, Proc. PowerGrid, Milan, Italy, 3-5 June 2008

8 Engineering Technical Report 124: ‘Guidelines for actively managing power flows associated with the connection of a single distributed generation plant’, Energy Networks Association, February 2004

9 Collinson, A., Dai, F., Beddoes, A., Crabtree, J.: ‘Solutions for the connection and operation of distributed generation’, DTI, July 2003

10 Roberts, D. A.: ‘Network management systems for active distribution networks – a feasibility study’, (SP Power Systems Ltd., Scottish Power Plc., 2004)

11 Scottish Hydro-Electric Power Distribution Limited: ‘Facilitate generation connections on Orkney by automatic distribution network management’, (Scottish and Southern Energy, 2004)

12 Currie, R. A. F., Ault, G. W., Foote, C., McDonald, J. R.: ‘Active power-flow management utilising operating margins for the increased connection of distributed generation’, *IET Proc. GTD*, 2007, **1**, (1), pp. 197–202

13 Dolan, M. J., Davidson, E. M., Ault, G. W., McDonald, J. R.: ‘Techniques for managing the power flows in active distribution networks within thermal constraints’, Proc. 20th Int. Conf. Electricity Distribution, Prague, CZ, 8–11 June 2009

14 Kabouris J., Vournas, C. D.: ‘Application of interruptible contracts to increase wind-power penetration in congested areas’, *IEEE Trans. Power Syst.*, 2004, **19**, (3), pp. 1642-1649

15 Castronuovo, E., Martinez-Crespo, J., Usaola, J.: 'Optimal controllability of wind generators in a delegated dispatch', *Electr. Power Syst. Res.*, 2007, **77**, (10), pp. 1442-1448

16 Makarov, Y. V., Loutan, C., Ma, J., de Mello, P.: 'Operational impacts of wind generation on California power systems', *IEEE Trans. Power Syst.*, 2009, **24**, (2), pp. 1039-1050

17 Yip, H. T., An, C., Aten, M., Ferris, R.: 'Dynamic line rating protection for wind farm connections', Proc. 9th Int. Conf. Developments in Power System Protection, Glasgow, UK, 17-20 March 2008

18 de Almeida, R. G., Castronuovo, E. D., Peças Lopes, J. A.: 'Optimum generation control in wind parks when carrying out system operator requests', *IEEE Trans. Power Syst.*, 2006, **21**, (2), pp. 718-725

19 Rodriguez-Amenedo, J.L., Arnalte, S., Burgos, J. C.: 'Automatic generation control of a wind farm with variable speed wind turbines', *IEEE Trans. Energy Convers.*, 2002, **17**, (2), pp. 279-284

20 Strah, B., Kujaca, O., Vukic, Z.: 'Speed and active power control of hydro turbine unit', *IEEE Trans. Energy Convers.*, 2005, **20**, (2), pp. 424-434

21 Siano, P., Ochoa, L. F., Harrison, G. P., Piccolo, A.: 'Assessing the strategic benefits of distributed generation ownership for DNOs', *IET Proc. GTD.*, 2009, **3**, (3), pp. 225–236

22 Wood, A. J., Wollenberg, B. F.: 'Power generation, operation and control' (Wiley, 1996), pp. 421-427

23 Zhou Q., Bialek, J. W.: 'Generation curtailment to manage voltage constraints in distribution networks', *IET Proc. GTD*, 2007, **1**, (3), pp. 492 – 498

24 Bialek, J. W.: 'Tracing the flow of electricity', *IET Proc. GTD.*, 1996, **143**, pp. 313–320

25 Kirschen, D., Strbac, G.: 'Tracing active and reactive power between generators and loads using real and imaginary currents', *IEEE Trans. Power Syst.*, **14**, (4), pp. 1312-1318

26 Payyala, S., Green, T. C.: 'Sizing of distributed generation plant through techno-economic feasibility assessment', *Power Engineering Society General Meeting*, October 2006

27 Strategic Environmental Assessment: 'Wind Background – Cost of Wind Power Generation', DECC, 2004, available: http://www.offshore-sea.org.uk, accessed March 2009

28 European Commission: 'Quarterly Review of European Gas and Electricity Prices', Luxembourg, 2005

29 Office of the Gas and Electricity Markets: 'Renewables Obligation: Annual Report 2006-2007', London, 2008

30 DTI: 'Offshore wind energy – Wind energy factsheet 1', London, 2001

31 DECC: 'Cost of and financial support for offshore wind', London, 2009

32 SP transmission and distribution: 'Distribution long term development statement for SP Manweb PLC for the years 2005/6 to 2009/10', SP Manweb plc, November 2005

33 Jantzen, J. 'Foundations of Fuzzy Control', (Wiley & Sons, 2007) pp. 35-36, 57-61

34 UK Meteorological Office: 'Data for the 'Valley' area of the UK', 2007, available at: http://www.metoffice.gov.uk, accessed January 2008

35 DTI: 'The electricity safety, quality and continuity regulations', The Stationery Office, 2002

36 Masters, C. L.: 'Voltage rise: The big issue when connecting embedded generation to long 11kV overhead lines', *Power Eng. J.*, 2002, **16**, (1), pp. 5-12

37 Hind, M., Jenkins, N. Taylor, P. C.: 'An active 11kV voltage controller: practical considerations', Proc. From 17th Conf. Electricity Distribution CIRED, Barcelona, 12-15 May 2003

38 Keane, A., Zhou, Q., Bialek, J. W., O'Malley, M.: 'Planning and operating non-firm distributed generation', *IET Proc. RPG*, 2009, **4**, (3), pp. 455 - 464

39 Michiorri, A., Taylor, P. C., Jupe, S. C. E.: 'Overhead line real-time rating estimation algorithm: description and validation', *Proc. IMechE Part A: J. Power and energy*, In press, 2009

Tables

Table 1 - DG scheme details

G_{id}	DG type	Installed capacity (MW)	Datum annual energy yield (GWh)
DG1	Onshore wind	24	30.9
DG2	Onshore wind	30	46.7
DG3	Onshore wind	39	71.5
DG4	Onshore wind	40	87.9
DG5	Onshore wind	56	114.6
DG6	Onshore wind	45	113.9
DG7	Offshore wind	90	205.5
DG8	Offshore wind	120	272.2

Table 2 - Component thermal ratings

Component	Static rating (MVA)	Average real-time rating (MVA)	Overhead line component properties
C1	89	n/a	Lynx 175mm^2 50^{o}C
C2	89	n/a	Lynx 175mm^2 50^{o}C
C3	89	139.6	Lynx 175mm^2 50^{o}C
C4	89	n/a	Lynx 175mm^2 50^{o}C
C5	89	141.6	Lynx 175mm^2 50^{o}C
C6	89	129.9	Lynx 175mm^2 50^{o}C
C7	89	128.3	Lynx 175mm^2 50^{o}C
C8	89	126.5	Lynx 175mm^2 50^{o}C
C9	120	177.9	Poplar 200mm^2 75^{o}C
C10	89	n/a	Lynx 175mm^2 50^{o}C
C11	89	n/a	Lynx 175mm^2 50^{o}C

Table 3 - Marginal aggregated DG annual energy yields

Control strategy	Marginal aggregated DG annual energy yields with different component rating systems (%)	
	Static	Real-time
LIFO trip	0.0	20.1
LIFO PFSF-based	6.5	20.5
Egalitarian	7.1	20.5
Technically most appropriate	11.0	21.0

Table 4 – Wind farm financial evaluation (static thermal ratings)

	Control strategy	Generator							
		DG1	DG2	DG3	DG4	DG5	DG6	DG7	DG8
NPV (£M)	LIFO trip	-0.9	5.9	16.9	29.9	34.6	46.5	49.0	64.4
	LIFO PFSF-based	19.8	30.2	48.9	67.2	79.0	80.3	154.8	216.0
	Egalitarian	40.5	48.2	62.6	72.2	72.1	72.3	161.2	190.4
	Technically most appropriate	49.2	58.6	76.2	85.5	61.7	53.6	150.9	187.4
PI	LIFO trip	-	0.2	0.5	0.9	0.8	1.3	0.5	0.5
	LIFO PFSF-based	1.0	1.2	1.5	2.0	1.7	2.2	1.7	1.8
	Egalitarian	2.0	1.9	1.9	2.2	1.6	2.0	1.8	1.6
	Technically most appropriate	2.4	2.3	2.4	2.6	1.3	1.4	1.7	1.6

Table 5 – Wind farm financial evaluation (real-time thermal ratings)

	Control strategy	Generator							
		DG1	DG2	DG3	DG4	DG5	DG6	DG7	DG8
NPV (£M)	LIFO trip	22.0	28.9	41.2	52.9	43.3	51.8	72.4	96.7
	LIFO PFSF-based	41.8	53.0	72.7	85.8	88.0	87.8	162.6	217.0
	Egalitarian	47.6	56.7	73.8	84.2	84.8	85.1	162.2	215.5
	Technically most appropriate	49.2	58.6	76.2	87.2	84.6	79.2	161.5	215.9
PI	LIFO trip	1.1	1.2	1.3	1.6	0.9	1.4	0.8	0.8
	LIFO PFSF-based	2.1	2.1	2.3	2.6	1.9	2.4	1.8	1.8
	Egalitarian	2.4	2.3	2.3	2.5	1.9	2.3	1.8	1.8
	Technically most appropriate	2.4	2.3	2.4	2.6	1.8	2.1	1.8	1.8

Figures

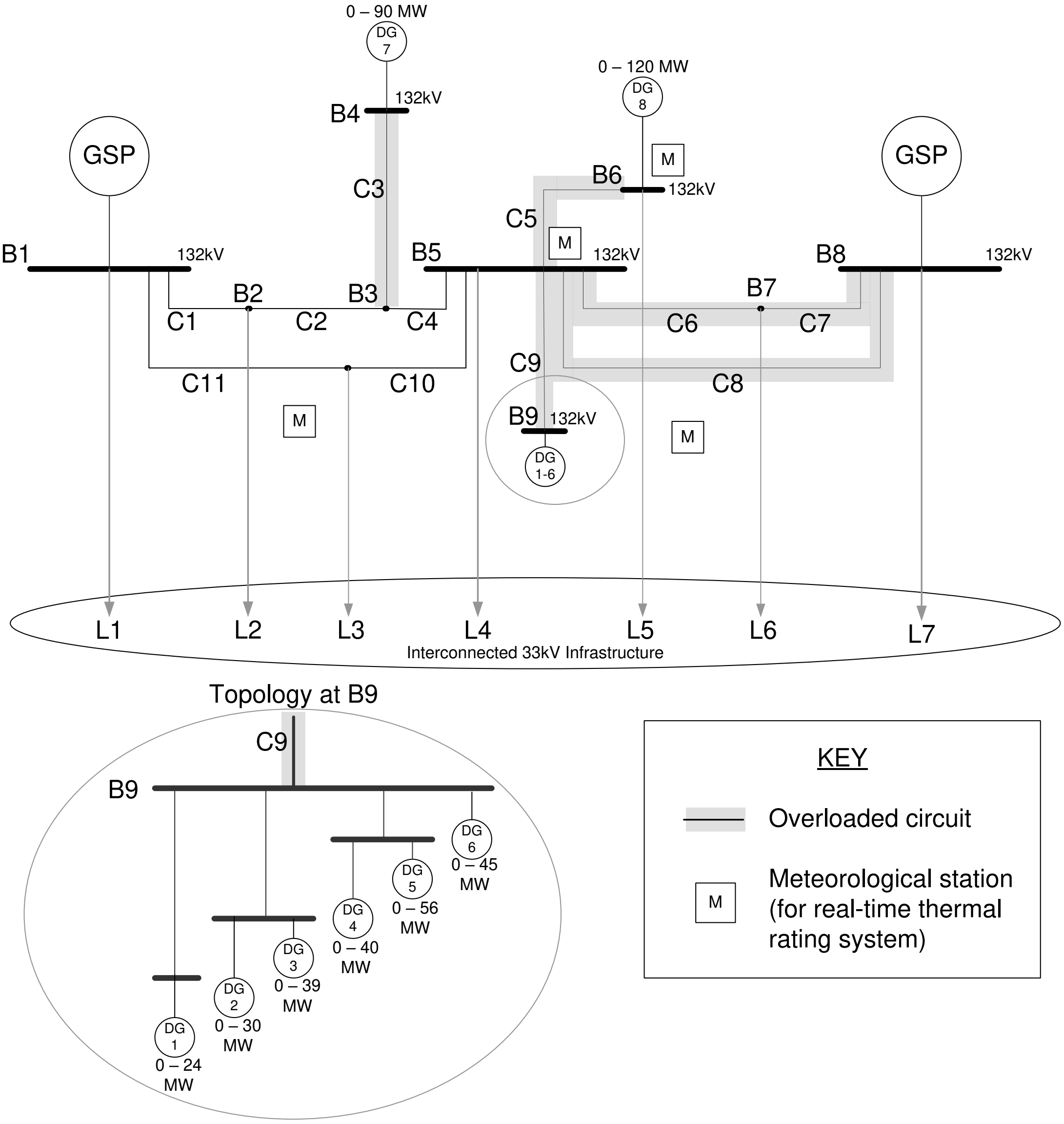

Figure 1. Field trial network topology

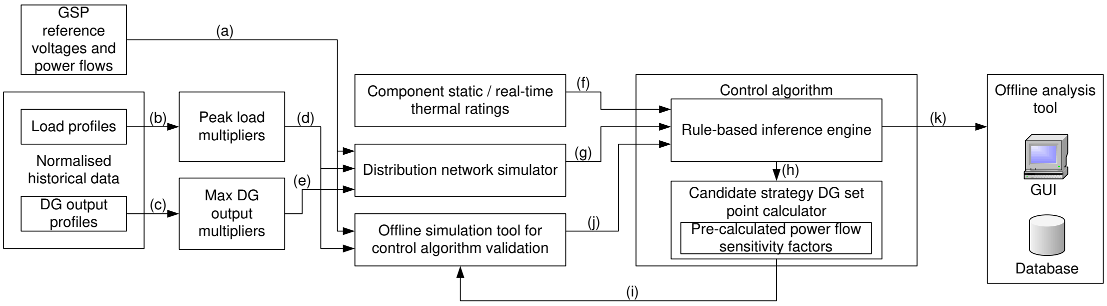

Figure 2. Power flow control block diagram

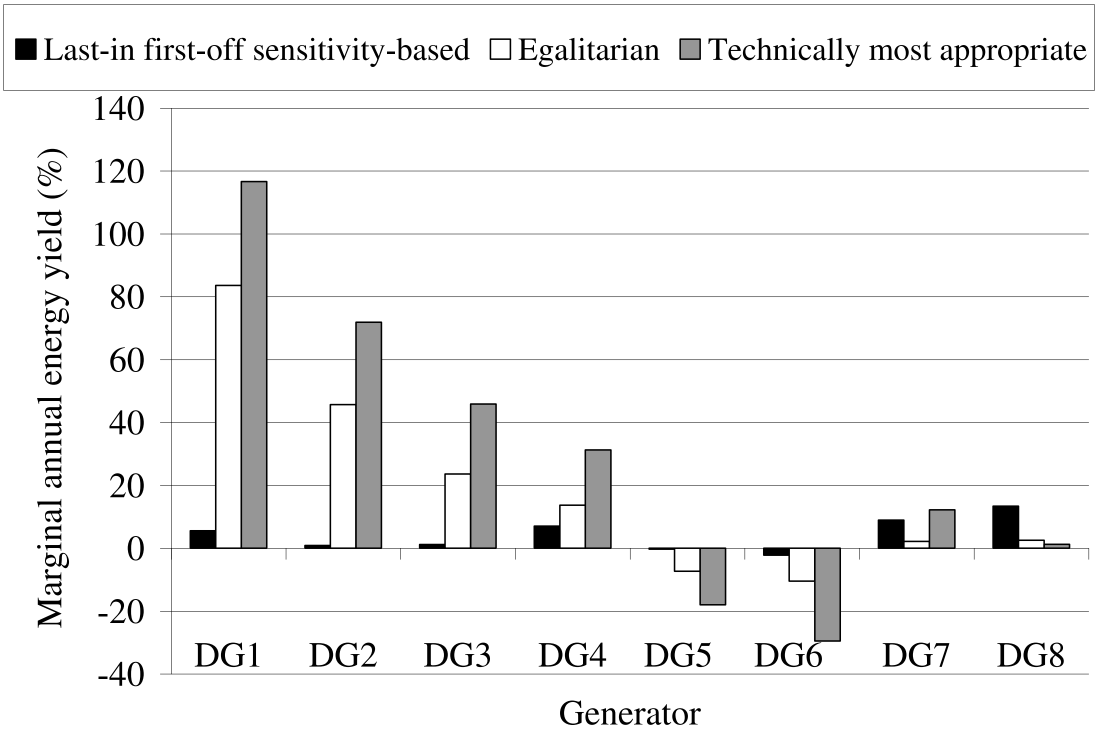

Figure 3a. DG marginal annual energy yields resulting from candidate control strategy deployments with component static thermal ratings

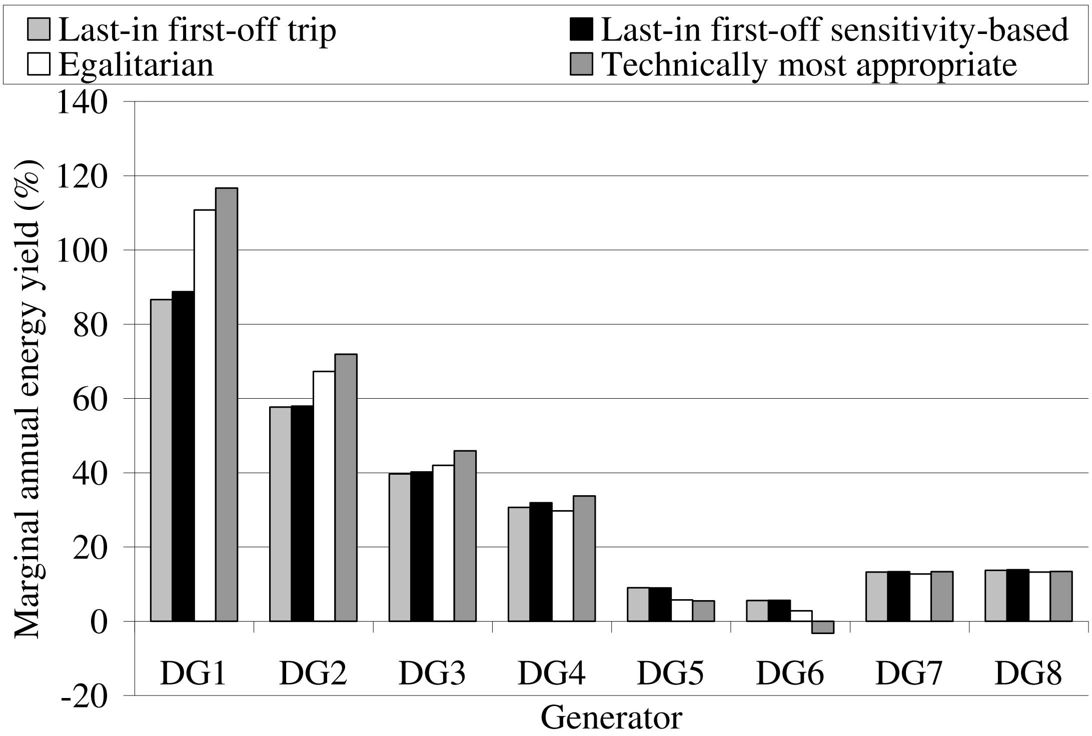

Figure 3b. DG marginal annual energy yields resulting from candidate control strategy deployments with component real-time thermal ratings

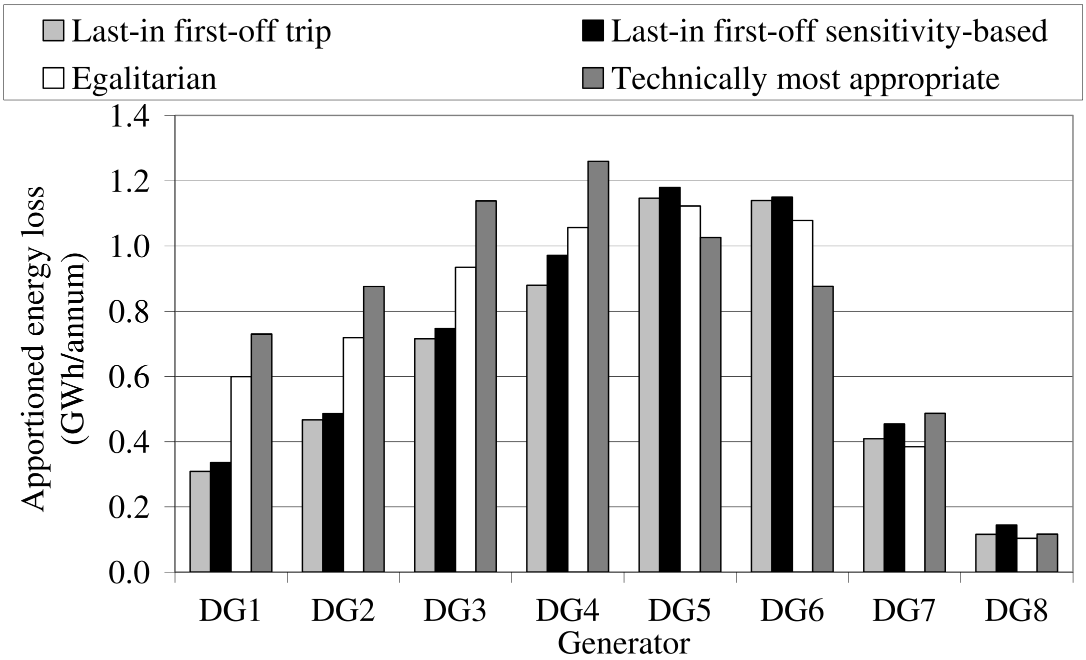

Figure 4a. DG apportioned annual energy losses resulting from candidate control strategy deployments with component static thermal ratings

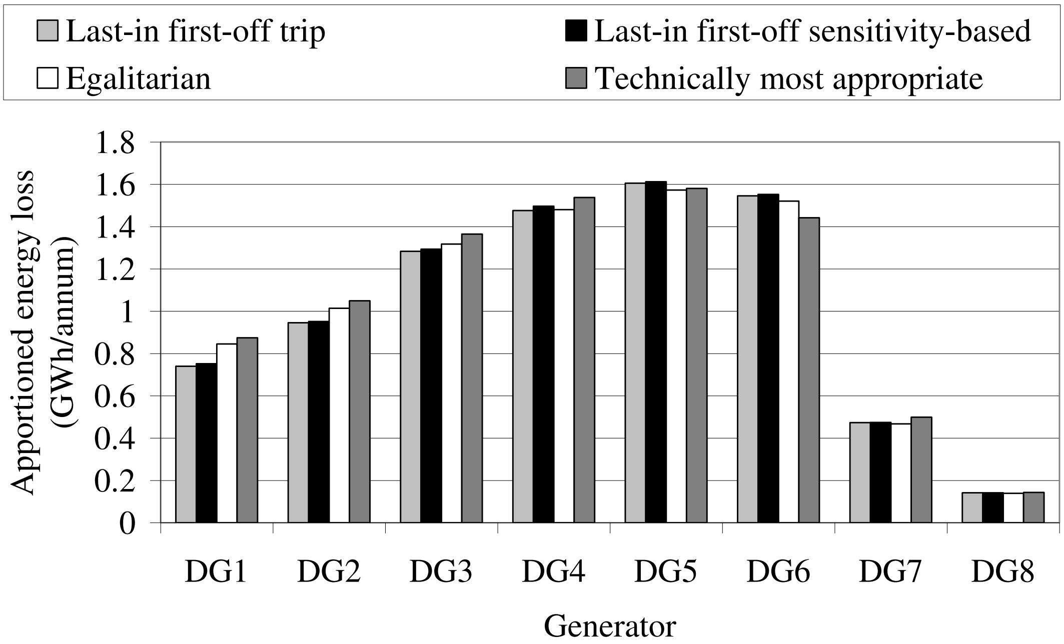

Figure 4b. DG apportioned annual energy losses resulting from candidate control strategy deployments with component real-time thermal ratings